

# *In situ* NMR and XRD studies of the growth mechanism of SBA-1†

C. C. Egger,‡<sup>a</sup> M. W. Anderson,\*<sup>a</sup> G. J. T. Tiddy<sup>b</sup> and J. L. Casci<sup>c</sup><sup>a</sup> Department of Chemistry, UMIST, Manchester, UK. E-mail: m.anderson@manchester.ac.uk;

Fax: +44 161 200 4559; Tel: +44 161 200 4517

<sup>b</sup> Department of Chemical Engineering, UMIST, Manchester, UK<sup>c</sup> Syntex, Johnson Matthey, Billingham, UK

Received 23rd December 2004, Accepted 16th February 2005

First published as an Advance Article on the web 17th March 2005

*In situ* <sup>17</sup>O, <sup>14</sup>N and <sup>29</sup>Si nuclear magnetic resonance (NMR) coupled with *in situ* energy dispersive X-ray diffraction (EDXRD) have been used to investigate the growth of the siliceous mesoporous material, SBA-1, synthesised under acidic conditions from a micellar solution of the surfactant hexadecyltriethylammonium bromide (HTEAB) and tetraethylorthosilicate (TEOS). For the last decade, the mechanism of growth of such materials has been thought to be driven by electrostatic interactions described as a co-assembly process between the silica species (I<sup>+</sup>) and the micelles (S<sup>+</sup>X<sup>-</sup>). However, this postulated model referred to as the “charge density matching model” has never been fully supported by experimental data for the acidic syntheses. We have carried out a detailed *in situ* study which challenges the so-called S<sup>+</sup>X<sup>-</sup>I<sup>+</sup> pathway and instead suggests that a salting-out effect coupled with a drastic change in the water activity are responsible for the composite I<sub>1</sub><sup>3</sup> (SBA-1 space group *P*<sub>6</sub>*m**3**n*) mesophase precipitation. Substantial reorganisation of the precipitated phase then results in the final structure.

## Introduction

Following the emergence of MCM-type *meso*-materials,<sup>1,2</sup> the SBA (Santa Barbara) series was first reported in 1994.<sup>3,4</sup> The synthesis of such materials depends upon the inorganic/organic interface which exists during synthesis, however, the mechanism associated with this self-assembly process has not been extensively studied. In particular, syntheses under highly acidic conditions, often found in SBA-type syntheses has received very little attention from a mechanistic viewpoint. Recently, we have shown that the structure of SBA-1 is a very low curvature surface formed from a high curvature surfactant micelle mesophase (see Fig. 1a and 1b).<sup>5</sup> The consequences are that the final structure is formed at the low curvature interface between silica and adsorbed water rather than silica and surfactant, thereby creating a structure with windows. In this work we monitor the kinetics of the processes which leads to this final structure.

The main synthetic difference between SBA mesoporous materials compared with the MCM family is the acidity of the medium. Changing pH changes the charge sign and nature of the inorganic species and consequently different materials are achieved. The SBA series is indeed different from the MCM series both in terms of structure<sup>6</sup> and robustness upon thermal treatment.<sup>3</sup> Both the MCM and SBA materials involve the growth of a silica structure within the aqueous zones of a surfactant mesophase. Because only moderate surfactant concentrations are employed, the mesophase must precipitate from solution at some stage during the reaction. To explain this, a model involving “charge density matching” has been generally accepted since 1994.<sup>3,4</sup> This model proposes that mesophases are precipitated from aqueous solutions due to strong electro-

static interactions between surfactant micelles, counter-ions, and charged inorganic species. It has had the great advantage of explaining the formation of all mesoporous materials. According to this mechanism, cationic inorganic species can react directly with anionic surfactant (S<sup>-</sup>I<sup>+</sup> pathway) or *via* the micellar counteranions of the positively charged surfactants (S<sup>+</sup>X<sup>-</sup>I<sup>+</sup> pathway). A similar route starting with anionic inorganic species is also proposed (the S<sup>+</sup>I<sup>-</sup> and S<sup>-</sup>M<sup>+</sup>I<sup>-</sup> pathways). Different types of mesophases have been obtained according to ref. 3.

The S<sup>+</sup>X<sup>-</sup>I<sup>+</sup> pathway (leading to SBA materials) has been reported to be supported by experimental evidence, summarised as follows:<sup>3,4</sup> (i) the formation of positively charged silica species at a pH below the isoelectric point (protonated silicic acids); (ii) a constant proton concentration during the synthesis; (iii) a 1 : 1 chloride-to-surfactant association ratio (hence the intermediate role given to the counter-ions); (iv) the easy removal of the template with ethanolic solution suggesting a neutral final skeleton; (v) the importance of the silica source in forming the *meso*-structure (if there is no hydrolysis occurring there is no mesophase produced, hence the assumption that I<sup>+</sup> species are crucial). However, none of these 5 experimental pieces of evidence unequivocally proves the model:<sup>4</sup> (i) the chemistry of silicas at negative pH has never been investigated, meaning that only assumptions at this stage can be made about speciation of silica at such low pH.<sup>7</sup> Moreover, between pH = 0 and 2, even though protonated silanols are postulated to explain the acid-catalysed hydrolysis of TEOS, they have never been detected experimentally;<sup>7</sup> (ii): there are no data to support the statement that the concentration of protons in solution remains constant. Moreover, the acidity of the medium can be excessively high (4.4 M HCl for a typical SBA-1 synthesis, giving a theoretical pH of about -0.7) such that pH measurements with a pH-meter no longer have any meaning. So, unless other techniques such as titrations are used to measure the concentration of protons, it is difficult to be sure of the constancy of proton concentration in solution; (iii) there

† Electronic supplementary information (ESI) available: Experimental data. See <http://www.rsc.org/suppdata/cp/b4/b419293c/>

‡ Current address: Institut de Science et d'Ingénierie Supramoléculaires, 8 allée Gaspard Monge, F-67083 Strasbourg, France.

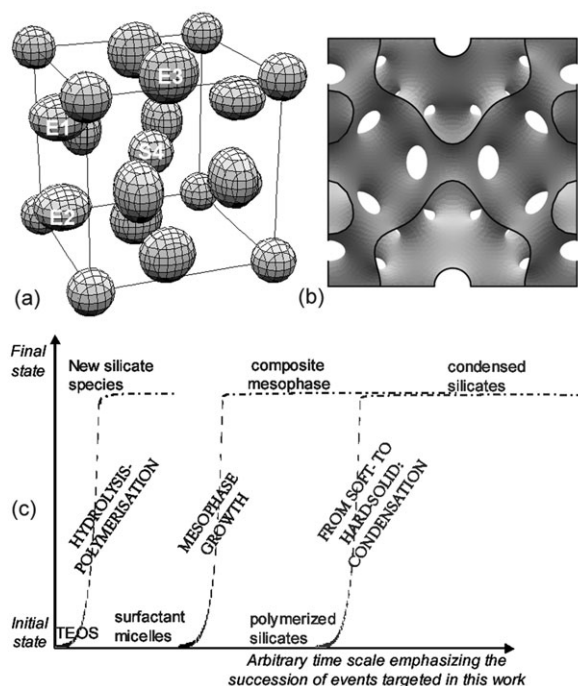


**Fig. 1** (a) Arrangement of spherical and oblate ellipsoidal micelles which make up the  $I_1$  cubic phase, space group 223. (b) Surface of the structure of SBA-1 which wraps around these micelles. (c) Schematic representation of the kinetics related to processes that may be involved in forming SBA-1 and targeted in this *in situ* work. The time scale is purposely arbitrary, it only gives an idea of the different processes sought.

are no data to support the 1 : 1 Cl : surfactant association. Moreover, the chloride anions are believed to act as intermediates between the cationic micellar surface and the cationic silica oligomers *via* H-bondings. Yet, it is known (ref. 8, p. 55) that chloride anions are not well solvated in water (only one molecule of water of solvation) and, consequently, it is difficult to agree with the concept that they could act as H-bridges between species; (iv) the easy removal of surfactant with ethanol has been reported subsequently by Ryoo's group in 1999.<sup>9</sup> However, they use an HCl–EtOH mixture rather than EtOH alone; (v) no experimental evidence is shown for the existence of  $I^+$  species.

Nearly all other mechanistic studies on the growth of mesoporous materials have employed basic conditions. This is the case, for instance, of all the *in situ* NMR work by Chmelka and co-workers<sup>10</sup> and the *in situ* EPR work by Galarneau *et al.*<sup>11,12</sup> When attempts are made to study the acidic mechanism (in film formation), it is under “soft” conditions.<sup>13</sup> A review published in 2002 gathering all the different types of *in situ* techniques used for monitoring mesophase growth has very little concerning work in acidic conditions.<sup>14</sup> This is probably due to the fact that the chemistry of silica solutions is not well known below pH = 0 which makes any mechanistic assumption really delicate. A recent paper from Tiemann *et al.* has opened a new pathway for studying *in situ* processes at low pH (3.9 M HCl) using *in situ* small-angle X-ray scattering (SAXS)<sup>15</sup> and a series of papers from Alfredsson *et al.*<sup>16,17</sup> use combined SAXS and  $^1\text{H}$  NMR to follow the preparation of mesoporous silicas in the presence of block-copolymer templates at low pH. There are some limitations to the techniques available to study these processes owing to the low concentration of reacting species. A typical surfactant/water molar ratio is 1 : 3500 and TEOS/water is 5 : 3500 for SBA-1 which makes  $^{14}\text{N}$  NMR or  $^{29}\text{Si}$  MAS NMR for instance, extremely challenging. For the same reason, the appearance of ordering as a function of time is difficult to access experimentally. This might be another reason why so

little *in situ* work has been published on SBA materials to corroborate the proposed  $\text{S}^+\text{X}^-\text{I}^+$  and  $\text{S}^-\text{I}^+$  pathways. Finally, simple DLVO considerations (see supplementary material)<sup>†</sup> would suggest that at such high salt concentrations where Coulombic interactions are almost entirely screened then charge matching pathways will be highly compromised.

### Choice of experiments: *in situ* NMR ( $^{17}\text{O}$ , $^{14}\text{N}$ , $^{29}\text{Si}$ ) and EDXRD

Fig. 1c gives a schematic of the processes which are targeted in this work: the initial hydrolysis of silica species; ordering of the surfactant phase and of the silica phase; condensation or cross-linking of the silica phase. The first process, hydrolysis and polymerisation of TEOS, is of interest as it is not reported in the literature at such low pH.<sup>7</sup> Thus, the acid-catalysed hydrolysis of silica plus the various degrees of polymerisation of these species need to be investigated, with and without the surfactant present, to account for the effect of the micelles on the silica chemistry. This is targeted by  $^{17}\text{O}$  NMR as  $^{17}\text{O}$ -species in the liquid state are easily and rapidly detectable using NMR. This is important as rapid hydrolysis cannot be followed with  $^{29}\text{Si}$  MAS NMR since the relaxation time for silicas is too large.

The rate of ordering within the mesophase is monitored by a combination of energy-dispersive X-ray diffraction (EDXRD) as well as  $^{14}\text{N}$  NMR. Finally, polymerisation and condensation of silicas are assessed with  $^{29}\text{Si}$  MAS NMR. The range of experiments performed are detailed in Table 1 with the composition of reagents given in Table 2.

## Experimental

### Surfactant preparation

The surfactant hexadecyltriethylammonium bromide (HTEAB) was prepared by mixing 1-bromohexadecane (98% Lancaster) and triethylamine (99% Jansen Chimica) in absolute ethanol under reflux conditions for 24 h. Ethanol is then removed with a rotary evaporator until a white, viscous paste is obtained. The resulting gel is recrystallised by a minimal addition of chloroform, and then ethyl acetate until the whole solid precipitates. The detailed procedure is described elsewhere.<sup>9</sup> Batch purity was then checked with  $^1\text{H}$  NMR (solvent chloroform-*d*) as well as microanalysis (C, H, N and Br). A purity of 97% is normally achievable.<sup>20</sup> Optical microscopy penetration scans using a polarised light optical microscope were also performed on HTEAB with water in order to have an approximation of the minimum temperature at which lyotropic liquid crystal phases occur. The solid surfactant placed between microscope slide and cover-slip is contacted with water which allows the observation of all the mesophases as distinct bands.<sup>18,19</sup> We report a detailed study of HTEAB phase behaviour elsewhere.<sup>20</sup>

### SBA-1 preparation

The silica-surfactant mesostructures were allowed to form under various time and temperature conditions, using TEOS (98% Aldrich) or TMOS (98% Aldrich) as a source of silica, our lab-made HTEAB, distilled water and aqueous HCl (33 wt% BDH). An optimum synthesis condition for SBA-1 is HTEAB:H<sub>2</sub>O : HCl : TEOS 1 : 3500 : 280 : 5. The details of the protocol are given in ref. 9. In order to perform these *in situ* experiments the ratios were sometimes modified (see Table 2) in order to optimise the experiment. When swelling of the SBA-1 phase was required for EDXRD experiments—as a tool to track changes in d-spacings—a 10 wt% bromohexadecane to HTEAB was added to the initial mixture (see Table 2). However, in all instances SBA-1 was formed at the end of the experiment. After a given ageing time at a given temperature

**Table 1** Range of experiments performed at various conditions of pH, temperature and composition

Experiment code	Experiments performed	pH	Temp./°C	HTEAB present	EDXRD batch code <sup>c</sup>	$\tau_{\text{batch code}}$ from EDXRD/min <sup>d</sup>	$\tau$ from <sup>17</sup> O/ min <sup>d</sup>	$\tau$ from <sup>14</sup> N/ min <sup>d</sup>
1	EDXRD <sup>b</sup>	-0.7	4	Yes	F, H	35 <sub>F</sub> , 30 <sub>H</sub>		
2	EDXRD, <sup>b</sup> <sup>17</sup> O, <sup>14</sup> N	-0.7	25	Yes	B, D, G, I	13 <sub>B</sub> , 25 <sub>D</sub> , 14 <sub>G</sub> , 15 <sub>I</sub>	1.4	13
3	<sup>17</sup> O	-0.7	25	No			3.7	
4	<sup>17</sup> O, <sup>14</sup> N	-0.7	60	Yes				
5	<sup>17</sup> O	-0.7	60	No				
6	EDXRD, <sup>b</sup> <sup>17</sup> O, <sup>14</sup> N, <sup>29</sup> Si <sup>a</sup>	0	25	Yes	C	?	17	60
7	<sup>17</sup> O, <sup>29</sup> Si <sup>a</sup>	0	25	No			50	
8	EDXRD, <sup>b</sup> <sup>17</sup> O, <sup>14</sup> N	0	60	Yes				
9	<sup>17</sup> O	0	60	No				
10	EDXRD, <sup>b</sup> <sup>17</sup> O, <sup>14</sup> N	1	25	Yes	E	?		
11	<sup>14</sup> N	1	60	Yes				
12	<sup>17</sup> O	1 + EtOH	25	Yes				
13	<sup>17</sup> O	2	25	Yes				
14 <sup>e</sup>	<sup>17</sup> O	1	25	No			> 500	
15 <sup>e</sup>	<sup>17</sup> O	2	25	No			> 500	

<sup>a</sup> Both TEOS and TMOS used as source of silicon. <sup>b</sup> Subsequently heated to 90 °C. <sup>c</sup> F, B (H<sub>2</sub>O/TEOS) = 140; H, D (H<sub>2</sub>O/TEOS) = 700; G has TMOS as source; I has additional swelling agent. <sup>d</sup> See text for explanation of  $\tau$ -value. Question mark indicates particles settle in reactor and consequently are not in X-ray beam. <sup>e</sup> Timescale much longer than duration of experiment. Error for D and H is  $\pm 5$  min and  $\pm 2$  min for other samples.

(high quality batches 1 week at 4 °C), the mixture is heated to 100 °C within 10 min for 1 h. The surfactant moiety is then burned out by calcination at 550 °C overnight, with a slow ramp rate (0.5 °C min<sup>-1</sup>). Samples were then characterised by powder X-ray diffraction.

### NMR spectroscopy

All NMR spectra were acquired at 9.4 T on a Bruker-MSL400 spectrometer. Measurements with H<sub>2</sub><sup>17</sup>O (Goss Scientific Instruments LTF, 10.46 at%) were collected in a specially designed vial (ca. 0.2 mL) positioned in a 10 mm Bruker static probe using a single pulse sequence with a recycle delay of 2 s and 128 scans. <sup>14</sup>N NMR measurements were carried out in home-made vials (ca. 1.5 mL) in a 10 mm Bruker static probe using a quadrupolar-echo pulse sequence, 90° pulses and 30  $\mu$ s interpulse delay, with a recycle delay of 0.5 s. Specially designed containers for both <sup>17</sup>O and <sup>14</sup>N allow identi-

cal positioning from one experiment to the next to avoid any shimming error. <sup>29</sup>Si NMR experiments were carried out in a 7 mm Bruker probe using a 7 mm rotor. Magic-angle spinning (MAS) *in situ* <sup>29</sup>Si measurements were performed on the silica-surfactant mixtures at 1 kHz. In all cases, single  $\pi/4$  were applied with proton decoupling during detection and 30-s recycle delays. <sup>29</sup>Si spin-lattice ( $T_1$ ) relaxation measurements were conducted using a saturation-recovery pulse sequence.  $T_1$  values of TEOS in water have been measured in this work to be 50 s, whereas  $T_1$  values of typical gels formed are 15 s for Q<sup>3</sup> species, and 58 s for Q<sup>4</sup> species. These parameters were chosen as a compromise recognising the very low concentration of silica and that there will be a slight emphasis of Q<sup>3</sup> over Q<sup>4</sup>. In all cases, there is an unavoidable error when starting the reaction, as there is a time gap between the addition of TEOS and recording the first spectrum. This time delay is 120 s but is negligible for the detection timescale of this experiment.

**Table 2** Molar quantities of components used for the various experiments performed. Some adjustment of molar quantities was made in order to suit the experimental technique

Experiment code	Experiment type	EDXRD batch code	pH	Temp./°C	HTEAB	H <sub>2</sub> O <sup>d</sup>	HCl	TEOS	TMOS	H <sub>2</sub> O TEOS or H <sub>2</sub> O/TMOS	TEOS/HTEAB or TMOS/HTEAB
2	<sup>17</sup> O		-0.7	25	20	2876	280	165	—	17	8
6	<sup>17</sup> O		0	25	174	17223	280	952	—	18	5
14	<sup>17</sup> O		1	25	—	155 680	280	7504	—	21	—
15	<sup>17</sup> O		2	25	—	1561 803	280	76 390	—	20	—
2	EDXRD	D	-0.7	25	1	3500	280	5	—	700	5
1	EDXRD	H	-0.7	4	1	3500	280	5	—	700	5
2	EDXRD	B	-0.7	25	1	700	56	5	—	140	5
1	EDXRD	F	-0.7	4	1	700	56	5	—	140	5
2	EDXRD	G	-0.7	25	1	700	56	—	5	140	5
2	EDXRD	I <sup>b</sup>	-0.7	25	0.9	700	56	5	—	140	5.5
6	EDXRD	C	0	25	1	700	17	5	—	140	5
10	EDXRD	E	1	25	1	700	1	5	—	140	5
2	<sup>14</sup> N		-0.7	25	1	505	53	5	—	101	5
6	<sup>14</sup> N		0	25	1	700	18	5	—	140	5
10	<sup>14</sup> N		1	25	1	812	1.5	4.8	—	169	4.8
6	<sup>29</sup> Si		0	25	1	700	13	5	—	140	5
6	<sup>29</sup> Si		0	25	1	700	13	—	5	140	5
7	<sup>29</sup> Si		0	25	—	700	13	5	—	140	—
7	<sup>29</sup> Si		0	25	—	700	13	—	5	140	—

<sup>a</sup> 10% enriched H<sub>2</sub><sup>17</sup>O was used for <sup>17</sup>O NMR experiments. <sup>b</sup> Additional 0.1 mol bromohexadecane swelling agent.

For  $^{17}\text{O}$  NMR measurements, owing to the small amount of TEOS in SBA-1 synthesis and to the potential difficulty to monitor silica species, the molar ratio  $\text{H}_2\text{O}/\text{TEOS}$  has been decreased from 700 to about 20. However, the ratio  $\text{TEOS}/\text{HTEAB}$  is maintained.

For  $^{14}\text{N}$  NMR measurement owing to the very dilute concentration of HTEAB in water in a typical SBA-1 synthesis and as a consequence to the related difficulty to detect  $^{14}\text{N}$  signal, the HTEAB concentration has been increased approximately 5 times along with that of TEOS.

For  $^{29}\text{Si}$  MAS NMR measurements concentrations were such that the gels are roughly 10 times more concentrated in TEOS (or TMOS) and HTEAB than in a typical SBA-1 synthesis. This is to enhance the signal to noise ratio of  $^{29}\text{Si}$  species. As there is no evidence of  $\text{Q}^0$  species even at early stages of reaction the spectra were added together on a time scale corresponding to 4 h (480 scans with a repetition delay of 30 s) in order to enhance the signal-to-noise ratio. After 24 h, the final gels left in the initial beaker were heated to  $100\text{ }^\circ\text{C}$  for 1 h, the resulting solids being filtered and dried at ambient temperature. X-ray diffraction was run on the final powders.

### Energy dispersive X-ray diffraction (EDXRD)

The energy dispersive diffraction method uses a white beam of X-rays; hence the wavelength,  $\lambda$ , becomes a variable. The detectors are positioned at desired angles,  $\theta$ , which are fixed. The measurements were carried out at Station 16.4 at CLRC Daresbury Laboratories (UK), following a similar set-up to that used and described in detail by O'Brien *et al.*<sup>21</sup> The main advantage of EDXRD is that there are no moving parts in the set-up: dynamic data collection is then simple and extremely rapid (resolution down to 1 s is achievable). Most importantly, in the SBA-1 synthesis stirring can be achieved in a similar manner to that used for normal SBA-1 preparations. The white energetic X-ray beam emerging from a synchrotron (20–150 keV) is very penetrating so that truly bulk samples can be analysed. However, the fast collection of data has its drawback: the quality of the diffraction pattern is intrinsically limited by the performance of the X-ray detector; the diffraction peaks are much broader than in standard scattering patterns. Consequently, if diffraction peaks are close together they are likely to overlap in EDXRD data.

Typically, a volume of *ca.* 15 mL of an SBA-1 mixture is placed in a simple stirred glass cell in front of the beam. The lowest angular detector collecting the X-ray of interest (large *d*-spacing) forms an angle  $2\theta$  of  $0.7^\circ$  with the incident beam. This angle is optimal for the type of work desired here, and consequently only data collected at this detector are presented. Patterns have typically been collected every 2 min. A heating and cooling facility (ethylene glycol bath) was available at the station and has been used to examine the effect of temperature on the kinetics of mesophase growth (from RT to low temperature for the ageing step) as well as in condensing the silicas upon temperature increase (condensation step). The temperature was directly measured within the cell with the use of a thermocouple. Using the ethylene glycol bath,  $90\text{ }^\circ\text{C}$  was the maximum temperature achievable and the temperature was never lower than  $4\text{ }^\circ\text{C}$ . When the concentration of TEOS is 5 times greater than it should be in a normal SBA-1 synthesis, the concentration of HTEAB is increased by the same ratio.

## Results and discussion

### Hydrolysis and polymerisation of TEOS: *in situ* $^{17}\text{O}$ NMR

Starting with the silicon alkoxide,  $^{17}\text{O}$  from  $\text{H}_2^{17}\text{O}$  is introduced into the silica species through hydrolysis. The location of  $^{17}\text{O}$  arises from the acid-catalysed hydrolysis and polymerisation mechanisms which are given in Fig. 2 for  $\text{pH} < 2$ ,  $\text{pH} = 2$  being the isoelectric point of  $\text{Si}(\text{OH})_4$ .<sup>7</sup> These two mechanisms

suggest that: (i)  $^{17}\text{O}$  is present only in water and silica species; (ii) ethanol molecules are formed throughout the process but do not contain  $^{17}\text{O}$ ; (iii) water molecules recovered at the end of a hypothetical full condensation will contain less  $^{17}\text{O}$  than at the beginning of the reaction.

Samples of SBA-1 have been prepared with and without the surfactant, from  $\text{pH} 2$  to  $-0.7$ , using the amounts of reactant given in Table 2. Fig. 3 gives the results for the experiments carried out at  $\text{pH} 0$  (3a and 3b) and approx.  $-0.7$  (3c and 3d) in the form of a 2D intensity plot (left), combined with the peak decay, both as a function time (right). At the end of the run carried out at RT, batches are kept for two weeks in a sealed vial before further study at higher temperature ( $60\text{ }^\circ\text{C}$ ).

Concerning the entire work carried out at RT, three observations can be made: (i)  $\text{pH}$  influences the chemical shift of the water peak; the chemical shift becomes less shielded as the  $\text{pH}$  value decreases. It typically varies from  $\delta = 0$  ppm ( $\text{pH} = 7$ ) to  $\delta \approx 2$  ppm ( $\text{pH} = 0$ ) and then to  $\delta \approx 10$  ppm ( $\text{pH} = -0.7$ ); (ii) as soon as TEOS is introduced in the vial, a decay in the  $^{17}\text{O}$  water peak is observed with time. It is this decay which contains the kinetic information of processes involved; (iii) no “ $^{17}\text{O}$ -silica” peak is observed unless small silica species are stabilised through addition of extra ethanol.<sup>22–24</sup> Upon heating, two trends are observed: (i) the chemical shift becomes more shielded at  $60\text{ }^\circ\text{C}$ , but the process is always reversible; (ii) there is a slight decrease in intensity of the signal that can be attributed to the Boltzman effect. A change in the shape of the peak is also observed and will be discussed later. Thus, intensity decay of the water peak is the only direct information that can be extracted from the full set of data.

At  $\text{pH} 1$  and  $2$  (data not shown), nothing happens to the water signal, the system is stable on the experimental time scale. Indeed, these two  $\text{pH}$  values are relatively high and too close to the isoelectric point of  $\text{Si}(\text{OH})_4$  ( $\text{p}K_i = 2$ ) for the hydrolysis and polymerisation to be rapidly acid catalysed. Such a high  $\text{pH}$  also does not yield SBA-1 due to the lack of reactivity of TEOS and hence no experiment has been carried out in the presence of surfactant under these conditions.

At  $\text{pH} = 0$  a decay is observed both in the presence and absence of HTEAB owing to the acid catalysed processes (Fig. 3a and 3b, respectively). However, the rate of the decay is substantially faster in the presence of HTEAB. These decays do not obey a simple exponential behaviour suggesting that more than one process is involved. However, it is possible to measure the shortest time at which the decay is almost complete. Without HTEAB it requires about 3000 s (50 min) for the water peak to decay to its minimum value, whereas with HTEAB only 1000 s are needed (about 17 min). The transformations that  $^{17}\text{O}$  in water undergoes, if similar, are three times faster in the presence of HTEAB. No  $^{17}\text{O}$  signal at higher

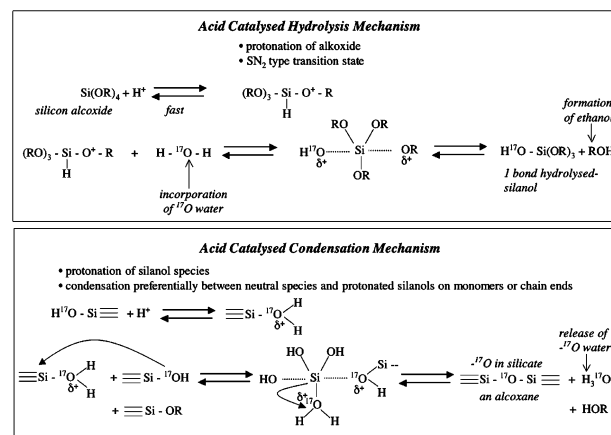
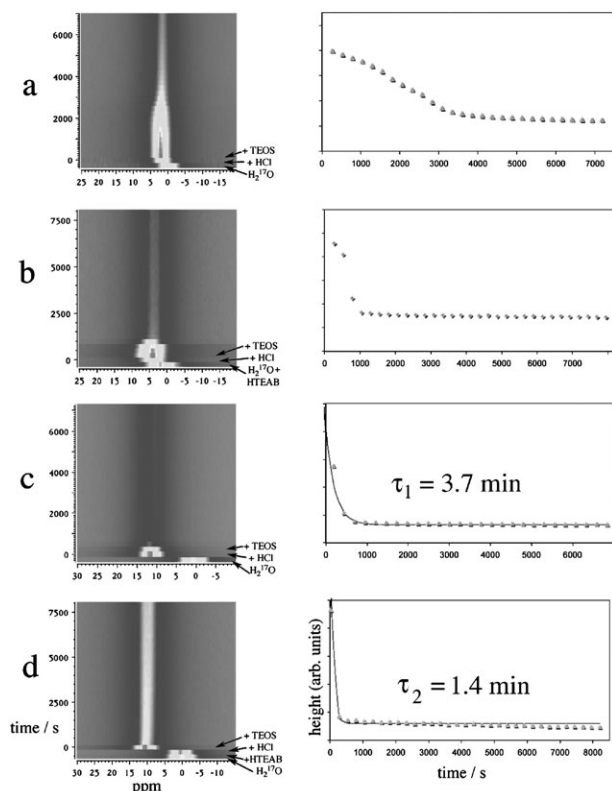


Fig. 2 Acid-catalysed mechanisms of hydrolysis and polymerisation of TEOS at  $\text{pH} < 2$ , emphasising the location of  $^{17}\text{O}$  in water and silica species.



**Fig. 3** Time-resolved *in situ*, room temperature,  $^{17}\text{O}$  NMR carried out at pH = 0 (a without surfactant, b with surfactant) and pH = -0.7 (c without surfactant, d with surfactant) showing the evolution in time of the water signal. A spectrum of 50  $\mu\text{L}$  of  $\text{H}_2^{17}\text{O}$  is inserted at the beginning of the series of 2-D data (line width is typically 170 Hz), as well as the spectrum of  $\text{H}_2^{17}\text{O} + \text{HCl}$  (and that of  $\text{H}_2^{17}\text{O} + \text{HTEAB}$  if applicable) in order to be able to compare the first peak after addition of TEOS with a reference.

chemical shift (in silica signal<sup>22–24</sup>) has been observed. At negative pH, with or without HTEAB, a large and fast decay is observed (Fig. 3c and 3d). This strongly supports the acid-catalysed mechanism. However, whereas the experimental decay without HTEAB is easily fitted with an exponential function (Fig. 3c), the fit is poor in the presence of surfactant (Fig. 3d). Again this suggests at least two different types of processes going on depending whether HTEAB is present or not. A time constant  $\tau$  characterising the transformations occurring in the case of TEOS at pH = -0.7 without HTEAB is of an exponential function type:  $I = I_0 \times e^{-t/\tau}$  with  $I_0$  the intensity at time 0 and  $\tau$  equals 3.7 minutes ( $\pm 0.5$  min, see Table 1). The time constant from the poor fitting of the experiment with HTEAB would be 1.4 minutes, about 2.5 times faster than without the organic moiety (it should be noted that the point at zero time is taken in the absence of acid to ensure that hydrolysis is not initiated).

The kinetics results shown at pH 0 and -0.7 are based only on the decay of the height of the signal as the line width is nearly constant. However, percentage losses are calculated more accurately from integration of the first (reference  $\text{H}_2^{17}\text{O}$ ) and last peaks and give the following results: at pH -0.7,

the loss is 57% [ $\pm 5\%$ ] without HTEAB, and 37% with HTEAB, whereas at pH = 0 the losses are, respectively, 35% and 51%. When  $\text{H}_2^{17}\text{O}$  molecules are used to hydrolyse TEOS,  $^{17}\text{O}$  is incorporated in the silica species (signal losses from the initial water signals are collected in Table 3). When these species start polymerising, they can lose their motion on the  $^{17}\text{O}$  NMR time scale, which renders part of the  $^{17}\text{O}$  signal “invisible”. Consequently, only a loss in the water signal is detected. However, the observed loss is always greater than can be accounted for by complete hydrolysis and consequently an additional process is occurring.

Correlating signal intensity loss in  $^{17}\text{O}$  NMR with the corresponding fate of the water molecules is not straightforward.  $^{17}\text{O}$  is a quadrupolar nucleus with spin 5/2. Consequently, there are 5 possible transitions all of which will be observed if the species undergo rapid reorientation (the rotational correlation time for free water is of the order of picoseconds and the quadrupole splitting is of the order of 7 MHz<sup>25</sup>). However, loss of mobility is liable to render all but the central transition ( $m_1 = -1/2 \rightarrow 1/2$ ) invisible. This could relate to bound-water molecules that are in exchange with free water at a rate slower than *ca.* 1/7 MHz, on the order of  $1.4 \times 10^{-7} \text{ s}^{-1}$  (in the same manner  $^{17}\text{O}$ -containing silica species with motion slower than  $1.4 \times 10^{-7} \text{ s}^{-1}$ , 7 MHz being a typical quadrupolar interaction for  $^{17}\text{O}$ .<sup>25</sup> This central transition represents 9/35 (*ca.* 25%) of the entire signal<sup>26</sup> and consequently if all the  $^{17}\text{O}$  nuclei had motion severely restricted then the NMR signal intensity would decrease to *ca.* 25% of its original value. In other words, if the signal decays by 75% then we must multiply this value by exactly 35/26 to determine the percentage of  $^{17}\text{O}$  with severely restricted motion ( $75\% \times 35/26 \approx 100\%$ ). As an example, at pH = -0.7 in the absence of HTEAB there is a 57% signal intensity loss which amounts to 77% of  $^{17}\text{O}$  with reduced mobility. If 23% of this is concerned with water consumed in the hydrolysis process then the remaining 54% must be related to “bound” water. Table 3 gives an analysis of the  $^{17}\text{O}$  results in terms of the amount of bound water. It should also be noted that even the central transition could be lost from second order broadening effects caused by severely restricted motion in solid-like components. This, however, seems unlikely as the changes to the  $^{17}\text{O}$  NMR spectrum occur when the solution is still clear and there is no evidence of solid precipitation.

A number of trends can be extracted from the  $^{17}\text{O}$  *in situ* work: (i) pH influences drastically the rate at which TEOS undergoes transformations; (ii) HTEAB increases the reaction rate (about threefold); (iii) the intensity loss in the  $^{17}\text{O}$  resonance will be associated with oxygen with reduced mobility a large fraction of which is most likely associated with substantial amounts of bound water.

No  $^{17}\text{O}$ -silica species have been detected on the time scale of the NMR experiment at the concentrations of TEOS used, whereas Babonneau *et al.*<sup>22–24</sup> observed them at slightly higher pH and in the presence of extra EtOH. Ethanol seems to stabilise silica species such as silicic acids and oligomers formed through hydrolysis and partial polymerisation. To confirm this, we carried out an experiment at pH = 1 in the presence of ethanol ( $\text{H}_2\text{O}/\text{EtOH} = 5$ , otherwise the same as experiment code 14 in Table 2). Silica species are detected at about 25 ppm,

**Table 3** Possible fate of water to account for loss of  $^{17}\text{O}$  NMR signal intensity. The signal loss is multiplied by 35/26 to determine the amount of  $^{17}\text{O}$  with restricted motion. This is then divided between water involved in hydrolysis and bound water

	pH = -0.7 no HTEAB	pH = -0.7 with HTEAB	pH = 0 no HTEAB	pH = 0 with HTEAB
% $^{17}\text{O}$ signal loss	57	38	35	51
% $^{17}\text{O}$ with restricted motion	77	51	47	67
% Maximum loss for hydrolysis	23	23	23	23
% Minimum associated with bound species	54	28	24	44

at early stages of the reaction, as a very weak hump beside the main water peak. At this chemical shift these species are expected to be silanols.<sup>24</sup> This simple experiment only proves that if silicas are not seen in the *in situ* work detailed above, it may only be related to their lack of mobility during the reaction instead of an experimental limitation, such as TEOS concentration ( $H_2O/TEOS \approx 20$ ).

### Mesophase growth: *in situ* EDXRD

Energy dispersive X-ray diffraction experiments were run varying pH, concentration, temperature of the initial mixture, as well as the presence or not of a swelling agent. Tables 1 and 2 summarise the set of 8 *in situ* experiments carried out, labelled batches B to I.

Fig. 4 shows the evolution of an EDXRD pattern (batch B) with time. From such a set of patterns, the growth is measured as the height of two diffracted peaks that grow with time (initially 38 and 42 Å). They are compared against the maximum height of the background around 26 Å. The *d*-spacings vary slightly with time and this variation has been followed during the mesophase growth. Batch SBA-1 E at pH = 1 has led to an amorphous powder (data not shown). No growth has been observed with EDXRD for this batch. At pH = 0, although no growth was easily observed, despite repetitive attempts, the XRD pattern of the final material SBA-1 C is characteristic of SBA-1 structure. The difficulty in monitoring the appearance of ordering at pH = 0 lies in the nature of the

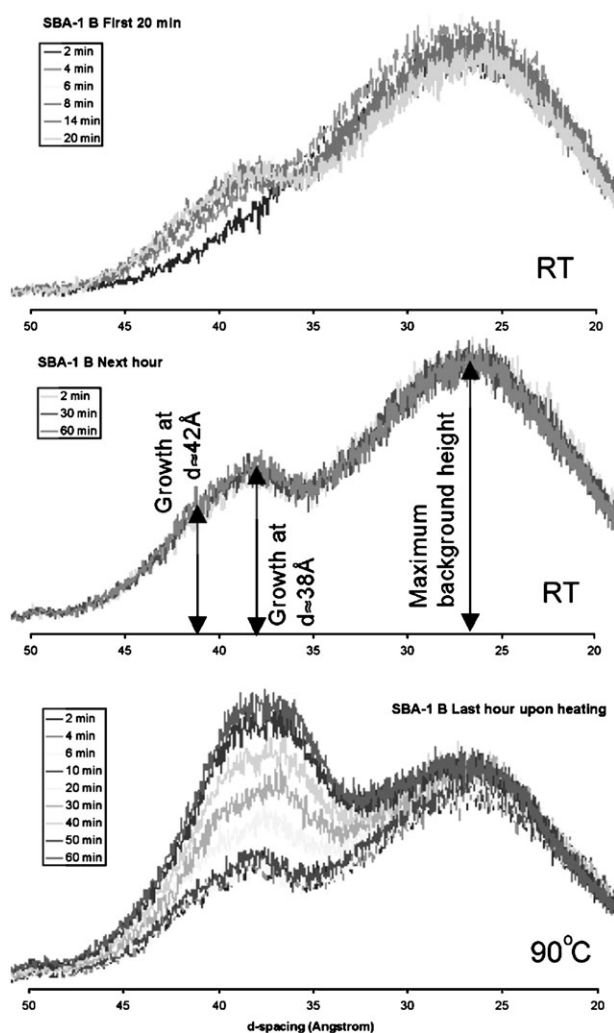


**Fig. 4** *In situ* EDXRD patterns of the SBA-1 batch B at initial, middle and final stages of the reaction. Growth is measured as the height of peaks emerging from the background at  $d = 38$  and  $42$  Å. These heights are compared to the maximum background height around  $d = 26$  Å.

particles formed. They are extremely “sticky” and readily settle at the bottom of the cell despite the stirring. Hence the particles are not in the X-ray beam. Fig. 5 presents the growth of the diffracted intensity as just defined as well as the evolution of the *d*-spacing as a function of time, for batch B, synthesised at pH = -0.7. Final batches of SBA-1 have been kept in their liquor solution during the time at Daresbury and then filtered and dried upon returning to the laboratory. XRD of the final powders have been recorded (data shown only for Batch B, as in inset in Fig. 5, other data are contained in the supplementary information†).

A number of observations come from these results: (i) at pH = -0.7 ordering occurs within 2 min and is already almost complete on the time scale of a few tens of minutes; (ii) diffraction intensity increases substantially with heating; (iii) *d*-spacings decrease slightly (*ca.* 2 Å lower) with increased temperature, due to an expected shrinkage of the structure upon heating.

In order to extract kinetic information from these results, growth curves for the two *d*-spacings tracked from time 0 to a time just before heating have been fitted with exponential functions. The result of the fits and the calculated exponential time constants are given in Fig. 6 for batch B. Errors on the heights of diffracted peak measurements have been estimated and are explicitly shown with the use of error bars. Accuracy is necessarily less in the case of normal concentration batches due to the smaller amount of matter used. From the full set of data for each batch, (Fig. 6 for batch B, other data shown in supplementary information†) the following information can be determined:

- Growth occurs roughly on the scale of 15 min at RT.
- The accuracy of the time constant,  $\tau$ , is different according to the concentration of constituents within the cell. (batches D and H  $\pm 5$  min, higher concentrations,  $\pm 2$  min).
- A 4 °C ageing step slows down the kinetics of mesophase formation by *ca.* a factor of 3 (compare  $\tau$  from B (*ca.* 13 min) with  $\tau$  from F (*ca.* 40 min)).

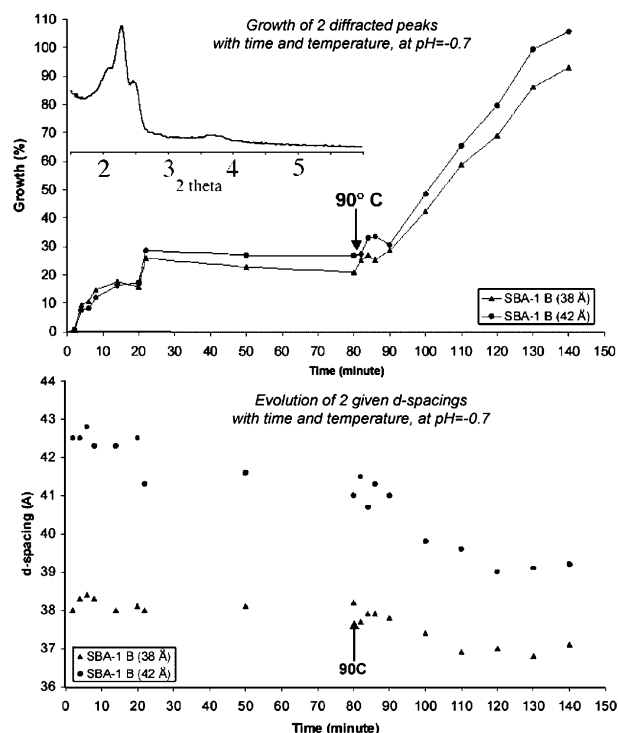


**Fig. 5** Above: Growth of two diffracted peaks with time, at RT and then upon heating to 90 °C for SBA-1 batch B. Inset: final XRD pattern of the resulting powder. Below: Evolution of the *d*-spacings with time at RT and then at 90 °C. Initial pH is -0.7.

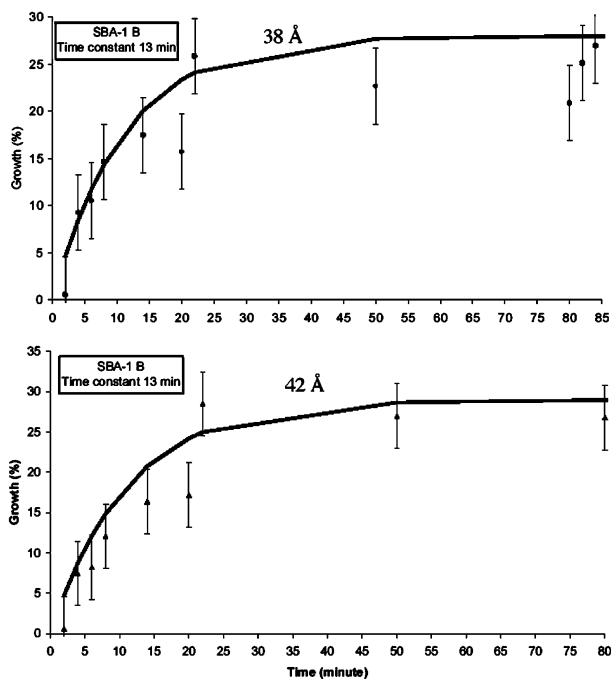


**Fig. 6** Time constants of growth extracted from exponential fits with experimental data before heating, for SBA-1 batch B, for two different  $d$ -spacings (38 and 42 Å).

(iv) The use of TMOS instead of TEOS, or of a swelling agent, does not seem to affect greatly the rate of SBA-1 ordering (14 min for G, 15 min for I vs. 13 min for B).

A summary of the final time constants determined from the raw data along with their uncertainty is given in Table 1. Two of the messages coming out of EDXRD results have their echo in the literature with the work from Tiemann *et al.*<sup>15</sup> which details the *in situ* SAXS study of meso-silica under acidic conditions: detection of the mesophase growth within 2 min and contraction of the mesophase with time and/or temperature.

### Mesophase growth: *in situ* $^{14}\text{N}$ NMR

*In situ*  $^{14}\text{N}$  NMR gives information about the local organisation of surfactant molecules as the reaction proceeds and can consequently help track mesophase formation. However, in this particular case, the  $^{14}\text{N}$  NMR tool is limited as the initial stage of the reaction contains an isotropic solution  $L_1$  (single line of width  $50 \pm 10$  Hz in  $^{14}\text{N}$  NMR) and the final product of the reaction is the  $I_1^3$  cubic phase, isotropic by nature (single line,  $100 \pm 10$  Hz, see supplementary information for  $^{14}\text{N}$  NMR spectra of water/HTEAB mixtures<sup>†</sup>).<sup>20,27</sup> Nevertheless, this line-width change is sufficient to use the maximum signal height as a kinetic probe of the onset of order. Tables 1 and 2 gather the different types of batches prepared for *in situ*  $^{14}\text{N}$  NMR work with three different conditions of pH studied. Owing to the very dilute concentration of HTEAB in water in a typical SBA-1 synthesis and as a consequence of the related difficulty to detect  $^{14}\text{N}$  signal, the HTEAB concentration has been increased *ca.* 5 times along with that of TEOS. It also renders *in situ* EDXRD and  $^{14}\text{N}$  NMR data directly comparable.

Only a single line is observed in these sets of *in situ*  $^{14}\text{N}$  NMR experiments. The height of the peak is plotted as a function of time for the three sets of spectra, recorded at pH = 1, pH = 0 and pH = -0.7 (Fig. 7 for the results at pH = 0 and pH = -0.7, pH = 1 is shown in supplementary information<sup>†</sup>). Insets with XRD patterns of the final materials are also included. Similar to the *in situ*  $^{17}\text{O}$  NMR and EDXRD experiments, transformations occurring are faster the lower the pH. Although a material with the meso-scale definition is

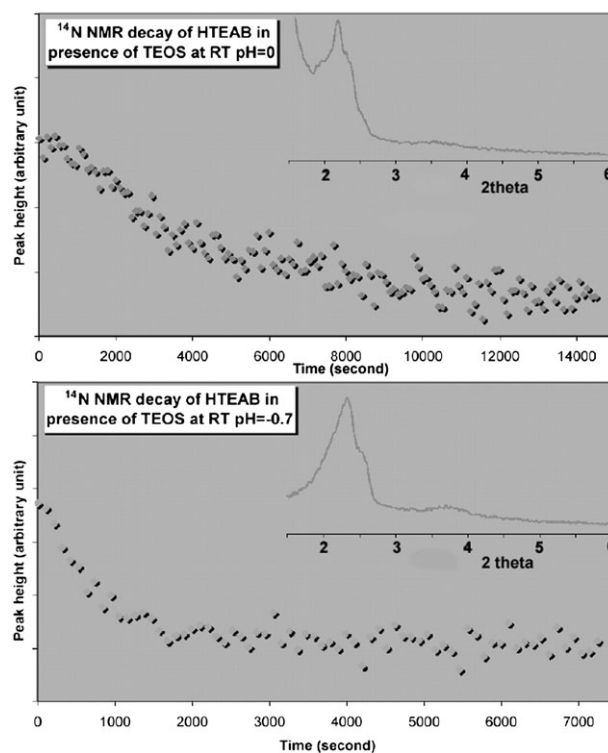


**Fig. 7** Decay of  $^{14}\text{N}$  NMR signal as a function of time for pH = 0 (above) and -0.7 (below). Insets: XRD patterns of the final materials.

formed at pH 1, this material remains particularly disordered (data not shown). However, XRD patterns of materials made at pH 0 and -0.7 are typical of SBA-1 structure. To avoid confusion about the decay of the peak and the amount of real loss in the signal, integrations of the first and last peak of the two sets of data (at pH = 1 the data are not shown) have been calculated to be: 2% at pH = 1, 67% at pH = 0, and 50% at pH = -0.7 (error  $\pm 5\%$ ).

The main information from the *in situ*  $^{14}\text{N}$  NMR work is that no obvious process is observed at pH = 1 after 4000 s, whereas a decay of the peak height is observed on this time scale at pH = 0, and a transformation occurs within 1000 s at pH = -0.7. These time scales, strongly connected with the pH values, are on the same order of magnitude as the ordering monitored with EDXRD experiments.

Both the  $^{17}\text{O}$  NMR and  $^{14}\text{N}$  NMR results show a similar trend although they cannot account for the same processes as they occur on different time scales: at pH = -0.7 a transformation is visible in the  $^{17}\text{O}$  signal within 2 min whereas a change is observed with the  $^{14}\text{N}$  NMR within 15 min. Yet, they both intrinsically contain information about *mobility* of species on their respective NMR time scale.

### Condensation: *in situ* $^{29}\text{Si}$ NMR

As SBA-1 forms, changes occur in the silica species which can be monitored with *in situ*  $^{29}\text{Si}$  MAS NMR with high power proton decoupling. Gels of different compositions have been studied at RT at pH = 0 with tetramethylorthosilicate (TMOS) or tetraethylorthosilicate (TEOS) as silica source. The idea is to compare their relative behaviour as their solubility in water is slightly different (TMOS is more soluble than TEOS). The experimental detail of the gels are summarised in Table 1. Results with TMOS or TEOS, either with or without the surfactant HTEAB are gathered in Fig. 8. Both resulting gels were dried and checked by X-ray diffraction, data not shown, revealing the SBA-1 structure. Owing to the low concentration of silica species, low sensitivity of  $^{29}\text{Si}$  and long relaxation times the spectra can only be collected over long time intervals—and

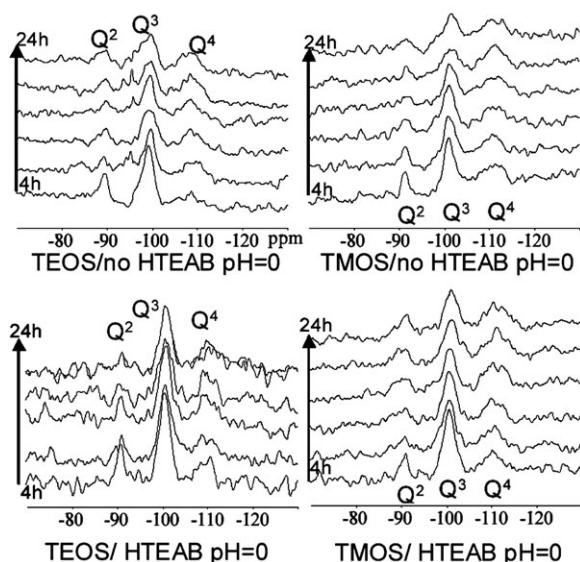


**Fig. 8** *In situ*  $^{29}\text{Si}$  HP MAS NMR spectra of TEOS/TMOS in water at pH = 0 with and without HTEAB, recorded at RT.

even then the spectra display considerable noise. Nevertheless, some observations are made as follows:

(i) At this pH, independent of the gel composition, there is relatively little  $\text{Q}^4$  species within the gel, indicating that the silica network is poorly condensed;

(ii) there is a decrease with time of  $\text{Q}^2$  and also  $\text{Q}^3$  species within the gels; however  $\text{Q}^3$  species remain predominant, whatever the gel composition;

(iii) there is no obvious difference between gels with TMOS as a silica source and those with TEOS;

(iv) there seems to be an influence from the HTEAB molecules to the degree of linkage within the gel: there are more  $\text{Q}^3$  species in the presence of HTEAB than without on the same time scale; this may simply be a result of the increased local concentration of silica species at the micelle surface, giving a more rapid reaction rate.

The  $^{29}\text{Si}$  NMR results confirm the trend reported in the literature that condensational cross-linking is not promoted at very low pH despite increased rates of hydrolysis. The degree of condensation is poor due to a preferential polymerisation between chain ends and monomers. As pH decreases the amount of  $\text{Q}^4$  species within the gel becomes less whereas  $\text{Q}^3$  species become predominant. From ref. 7 it is known that oligomers formed by an acid-catalysed mechanism remain small: up to seven silicon atoms only at 0.05 M HCl (pH  $\approx$  1.3). At this stage, the detailed speciation of silica is required in order to have a clearer idea of what is actually interacting as the phase grows and in this respect mass spectrometry might be useful in the future.

### The mesoporous material formation mechanism

It is known from surfactant chemistry that upon addition of electrolyte to a solution the solubility of the solute becomes affected such that a concentrated surfactant phase (containing ca. 50 wt% water) precipitates from the aqueous phase. This is known as the salting-out effect. One simple way to explain this effect is to consider the solvation of the introduced ions as each ion requires a certain number of molecules of water as a solvation sheath. Because the ions are usually small they are easily and preferentially solvated. At high electrolyte concentration, there are so many ions in the system that a large number of water molecules serve to hydrate them. Consequently, these are no longer available for solvating other species present in solution, particularly those that are only weakly solvated. Hence, the solubility of weakly solvated

solutes drastically decreases and the aqueous solutes can precipitate out from the dilute aqueous phase. This explanation would be extremely useful if it could be applied to the case of SBA-1. Indeed, in a typical SBA-1 synthesis the concentration of HCl is 4.4 M making salting out effects extremely likely: although  $\text{Cl}^-$  ions are poorly hydrated (one water molecule per anion),  $\text{H}_3\text{O}^+$  has three water molecules of hydration, ref. 8, p. 55. Hence,  $3 \times 4.4$  moles of water are used to hydrate the protons from the 55 available (in one litre of solution). So 13.2 moles of water are used to solvate protons alone, to which 4.4 must be added to account for solvation of  $\text{Cl}^-$ . Then, 1/3 of the water (in moles) is used for hydration of HCl and is no longer available for solubilising the micelles. This will change a great deal the micellar solubility so that the micelles arrange themselves in a concentrated phase where less water is required. It is known<sup>28</sup> that alkyl( $\text{C}_{12-16}$ )tributylammonium bromides show this type of partial miscibility above a certain temperature when added inorganic electrolytes increase the phase separation. Thus, this family of tetra-alkyl ammonium surfactants is prone to such behaviour. It is an indication that only a small change in the interactions between the surfactant micelles can result in phase separation. However, attempts to precipitate the  $\text{I}_1$  phase from a dilute solution of surfactant only with high concentrations of HCl have always been unsuccessful. Yet, since a mesophase does precipitate when a source of silicon alkoxyde is present it means that silica species play a crucial role in the overall solubility of the system.

The precipitation of an ordered mesophase occurs on the same time scale whether monitored with EDXRD or  $^{14}\text{N}$  NMR. An  $\text{I}_1$  phase is formed, to the detriment of other phases which can be described with the concept of water activity. When the  $\text{I}_1$  phase forms it must have the same water activity (or chemical potential) as that of the dilute aqueous phase within which it is dispersed. The water activity depends on the "free" water concentration. Water activity changes throughout a phase diagram of a surfactant in water, decreasing monotonically as the surfactant concentration is increased. Phases at low water-content have lower water activity than those at high water content (a lamellar phase has a lower water activity than a hexagonal phase). A micellar solution has high water activity since it has the lowest surfactant concentration. A schematic representation of this effect throughout the partial phase diagram of HTEAC is given in Fig. 9a. The reduction in water activity with concentration can be represented as arising from repulsions between the micelles.<sup>28-32</sup> When a concentrated phase coexists with a dilute one, the water activity is the same in both—hence the water activity is constant in the two-phase region. The concentrated phase has smaller repulsive interactions between the micelles than would normally be expected—*i.e.* there is an additional inter-micellar attractive force. Thus, in the  $\text{L}_1 + \text{I}_1$  region, where the initial stages of SBA-1 formation occur, there must be an additional attractive interaction between the micelles in the concentrated phase. We suggest that this arises from the presence of the silica oligomers (as illustrated in Fig. 9b). In some way these must "cross-link" adjacent micelles to provide the attractive interaction (see below). The partition of water in the system can be observed by  $^{17}\text{O}$  NMR: the chemical shift changes with pH—data not shown—suggesting a strong solvation of the protons by the water molecules, unshielding the magnetic field that  $^{17}\text{O}$  now experiences. Moreover, at 60 °C, as the overall system becomes more mobile, two types of signal are detected strongly suggesting two types of water, silicate-bound water and  $\text{H}^+$ -solvation water. When the partition is such that the system equilibrates, the system is precipitated out: it has reached a point at which the water activity is equal to that on an  $\text{I}_1$  phase. The  $\text{I}_1$  phase forms as the silicate polymerises.

The loss of signal intensity of both  $^{17}\text{O}$  and  $^{14}\text{N}$  demonstrates that relatively slow molecular motions of both water and surfactant develop as the reaction proceeds, but that they

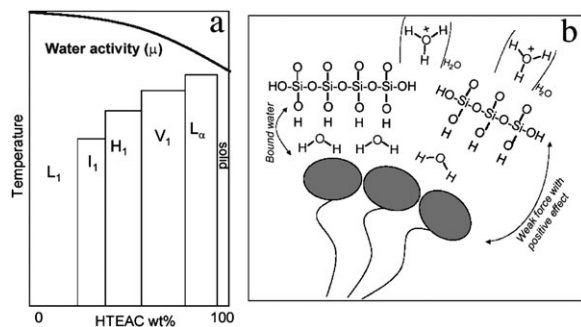


**Fig. 9** (a) Simplistic representation of the change of water activity within the schematic phase diagram of HTEAC. (b) Partition of water due to a salting-out of the composite silica–surfactant mesophase from the highly concentrated solution of HCl (4.4 M), coupled with a loss of water mobility from binding to the silica species.

occur on different time scales. For the water, this slow motion must arise from binding to the silica polymerising species produced in the first seconds/minutes of the reaction. Thus, the  $^{17}\text{O}$  signal loss is due to a broadening of the satellite quadrupolar transitions for the bound water; this then exchanges rapidly on the NMR time scale with free water. The signal loss is not from 100% of the water, indicating that the silica species are too dilute for all the water to contact the silica species on the time scale concerned. The fraction of  $^{17}\text{O}$  signal lost is smaller in the presence of HTEAB at  $\text{pH} = -0.7$ , indicating that less water can access the silica species. Thus, these species are present in larger units, since the surfactant is unlikely to influence directly the free-bound water exchange process. The surfactant micelles bind silica polymerising species, long before the loss of  $^{14}\text{N}$  intensity is observed.

The  $^{14}\text{N}$  signal loss is due to a broadening of the quadrupolar transitions because of slow molecular motions; in this case the motions are those that result in the 3D averaging of the net electric field gradient at the  $^{14}\text{N}$  nucleus. The motions that do this are the overall rotation around the surfactant micelles and the tumbling of the micelles themselves. We observe that the loss of the  $^{14}\text{N}$  intensity occurs on the same timescale as the growth of X-ray peaks at 38 and 42 Å. These peaks reflect the growth of the ordered mesophase precipitate, containing both silica and surfactant. Within this precipitate at least some of the surfactant head group motions within micelles become slow on the NMR time scale. Note that this precipitate does not have a fixed structure, but must be labile—at least in the early stages. When the micelles come together we do not know their size. In the final SBA-1 solid there are micelles of two different sizes. These must form in the first stages of the precipitate because when polymerisation is well advanced the structure will be too rigid to allow the necessary holes within the network. When considering the loss of  $^{14}\text{N}$  signal intensity we must consider the two types of micelle separately (see Fig. 1). The disc micelles can not undergo isotropic rotation because they are “locked” in the cubic mesophase lattice, thus will give a quadrupole splitting. The spherical micelles could give a sharp NMR line, provided the diffusion of monomers around the micelle is fast enough ( $< ca. 10^{-5}$  s). Assuming a micelle radius of  $ca. 2.3$  nm, this requires a self-diffusion coefficient  $D > 3.4 \times 10^{-12} \text{ m}^2 \text{ s}^{-1}$  [ $D = l^2/6t$ ]. The normal self-diffusion coefficient for surfactant within a micelle is expected to be  $ca. 10^{-10} \text{ m}^2 \text{ s}^{-1}$ . Given that the silica polymer does not have free rotation ( $D = 0$ ), it seems reasonable that the micelles separated from this surface by only a few water layers could have this reduced diffusion rate. The fraction of signal lost ( $ca. 60\%$ ) is consistent with slow motions for both types of micelles.

In the initial stages of the precipitation it is unlikely that the  $L_1$  phase contains two different micelles in the necessary proportions and of precisely just the size required to fit into

the  $I_1$  phase. After the initial hydrolysis of the TEOS (or TMOS) the oligomeric silica species bind to the micelle surface, probably being located between the head groups close to the hydrophobic interior (in the “palisade layer”). Here they can become cross-linked, and eventually provide the inter-micellar attraction leading to precipitation of a concentrated surfactant phase. Thus the concentration of silica solubilised in the precipitate is likely to be at least half that of the surfactant. Initially, this precipitate might be a disordered micellar phase, rather than an  $I_1$  structure. Note that compared to the material formed at  $\text{pH} = -0.7$ , the precipitate formed (more slowly) at  $\text{pH} = 0$  is far less ordered. This may be because the slow formation leads to a more polydisperse mixture of silica oligomers, with differing stages of polymerisation and condensation. The precipitate phase at  $\text{pH} = -0.7$  rapidly becomes more condensed and loses water. The water loss, possibly resulting from the reduced water-binding of silica polymers because the SiOH groups are removed, leads to an increased surfactant concentration in the phase, resulting in the formation of the  $I_1$  structure. Hence, the  $I_1$  formation is probably a two-stage process. [Precipitation of a concentrated amorphous phase, structuring within the amorphous phase to form  $I_1$ ]. From the  $^{29}\text{Si}$  NMR data, we see that the silicas formed are not highly condensed, thus there is access for water binding which is reduced as the polymerisation becomes complete. The higher concentration of  $Q^3$  species in the presence of surfactant probably arises from the enhanced concentration of the silica around micelles, leading to a faster reaction.

Recently, we have shown that the final structure of SBA-1 is a very low curvature surface formed from a high curvature surfactant micelle mesophase.<sup>5,33</sup> Consequently, as the order of the silica develops the silica must retract from the intermicellar region in order to create windows. The final interface will be the low curvature interface between the silica and the water rather than between the silica and the surfactant. This is not surprising as the silica becomes more hydrophobic upon polymerisation and also water is produced as the silica condenses. Both these facts will serve to preferentially solvate the surfactant with water in the later stages of synthesis producing a bound water layer on the surfactant. A similar process must be in operation for other cage-like mesoporous materials where windows are formed such as SBA-6, SBA-12 and SBA-16.

Thus the mechanism is:

1. Fast formation of silica hydrolysed species—fast binding to micelles.
2. Slower aggregation of these to form an amorphous precipitated phase.
3. Further development of order within the precipitate as the polymerisation continues to form the  $I_1$  structure.
4. Movement of the silica network away from the micellar surface to be fully located in the water region between micelles with the consequent formation of windows.

A general and final representation of the succession of events in the mechanism accompanied with their time scale is displayed in Fig. 10.

This raises the question of the molecular mechanism by which the initial silica species bind to the micelles. From DLVO considerations a charge interaction model seems unlikely. A related question is: why do the micelles catalyse the polymerisation reaction? Presumably, the micelles also bind  $\text{H}_3\text{O}^+$  because this is the only way to catalyse the polymerisation. Thus the concentration of silica and acid are both higher at the micelle surface than in the bulk. Because of the speed of hydrolysis it is unlikely that any TEOS is solubilised within micelles. Further polymerisation of the silica leads to cross-linking of micelles, followed by development of the X-ray patterns. At this stage the two sizes of micelles are present.

Further development of the polymerisation process will reduce the silica water binding—and the location/strength of silica binding to the micelles. When this happens, the structure

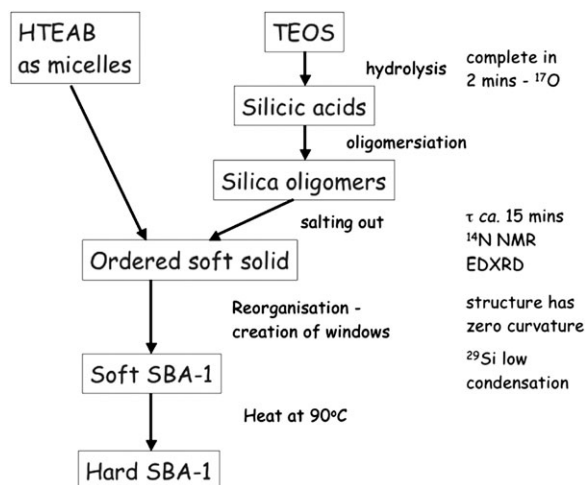


**Fig. 10** General kinetic picture representing the different steps involved in forming SBA-1. TEOS is rapidly hydrolysed (complete within 2 min) to silicic acid species that start polymerising, preferentially linearly ( $\tau \approx 1.4$  min). As they polymerise, water molecules lose mobility and bind to their surfaces. This effect coupled to the salting-out effect due to the presence of 4.4 M HCl induces the composite mesophase precipitation ( $\tau \approx 15$  min). An ordered soft solid is formed, which then rearranges to create windows between cages. Further condensation occurs to produce a hard solid upon heating to 90 °C.

is so far developed that it is impossible for the micelles to escape from the silica framework. The restricted molecular mobility and the physical presence of the silica will reduce the micelle exchange kinetics.

At this stage the silica becomes too condensed to interact with the surfactant head groups. So the head groups are solvated by water (and  $\text{H}_3\text{O}^+$ ) hence the silica moves as far from them as it can—to the interstices between the micelles—hence the “windows” between micelles develop at the points of closest micellar contact. The development of windows and their dimensions must be determined in part by the volume fraction of silica in the precipitated phase. It is unlikely that significant concentrations of silica can diffuse into the precipitated phase after its formation. From previous modelling studies<sup>5</sup> we estimate the volume fraction of silica in the non-calcined material to be 42%. In typical surfactant systems the  $I_1$  cubic phase in equilibrium with a micellar solution contains of order 40–50% surfactant (by volume or weight). This is likely to hold here. Thus the  $I_1$  precipitate must contain (at most) 15–20% water [including electrolyte/acid]. This will be distributed between the surfactant head groups and silica species, filling the volume between the micelles. From these considerations we see that the micelles must be completely covered with silica oligomers, hence it will be easy for cross-linking of micelles to occur. Additionally, as the condensation proceeds, it seems likely that silica binding to the micelles is reduced because water and surfactant are excluded from the condensed silica. As the silica shrinks it occupies the spaces furthest from the micellar surfaces. Finally, we comment on the fact that regular windows do not occur in other materials such as MCM 41 where the rod micelles are fully encased in the surrounding silica structure. Either there is a much larger fraction of silica in the precipitated hexagonal phase in the case of the MCM 41, or the (intermicellar) surface area of the SBA-1 structure is too large to be covered by silica.

## Conclusion

In conclusion, we establish the timescale of some of the key processes in the formation of SBA-1 under highly acidic conditions. Initial hydrolysis of the silica source occurs on a

timescale of about 2 min and is accompanied by a binding of water to small oligomers. This reduction in water activity results in salting out of an ordered silica/water/surfactant mesophase on a timescale of around 15 min. The silica remains highly fluid which permits substantial rearrangement of the silica, retracting from the micelle interface and forming windows in the final SBA-1 structure.

## Acknowledgements

The authors would like to acknowledge technical support at Station 16.4 at CLRC Daresbury for help to set up the EDXRD experiments. Phil Hughes is also warmly thanked for his dedicated time at the station. Thanks to John Ridland at ICI Syntex for the original idea to perform  $^{17}\text{O}$  NMR experiments. Thanks also to ICI Syntex for financial support.

## References

- C. T. Kresge, M. E. Leonowicz, W. J. Roth, J. C. Vartuli and J. S. Beck, *Nature*, 1992, **359**, 710–712.
- J. S. Beck, J. C. Vartuli, W. J. Roth, M. E. Leonowicz, C. T. Kresge, K. D. Schmitt, C. T.-W. Chu, D. H. Olson, E. W. Sheppard, S. B. Mc Cullen, J. B. Higgins and J. L. Schlenker, *J. Am. Chem. Soc.*, 1992, **114**, 10834–10843.
- Q. Huo, D. I. Margolese, U. Ciesla, D. G. Demuth, T. E. Gier, P. Sieger, A. Firouzi, B. Chmelka, F. Schüth and G. D. Stucky, *Chem. Mater.*, 1994, **6**, 1176–1191.
- Q. Huo, D. I. Margolese, U. Ciesla, P. Feng, T. E. Gier, P. Sieger, R. Leon, P. M. Petroff, F. Schüth and G. D. Stucky, *Nature*, 1994, **368**, 317–321.
- M. W. Anderson, C. C. Egger, G. J. T. Tiddy, J. L. Casci and K. A. Brakke, *Angew. Chem.*, 2005, **44**, in press.
- M. Kruk, M. Jaroniec, R. Ryoo and J. M. Kim, *Chem. Mater.*, 1999, **11**, 2568–2572.
- C. J. Brinker and G. W. Scherer, *Sol-Gel Science*, Academic Press, New York, 1990.
- J. Israelachvili, *Intermolecular and Surface Forces*, Academic Press, New York, 1992.
- M. J. Kim and R. Ryoo, *Chem. Mater.*, 1999, **11**, 487.
- A. Firouzi, F. Atef, A. G. Oertli, G. D. Stucky and B. F. Chmelka, *J. Am. Chem. Soc.*, 1997, **119**, 3596.
- A. Galarneau, F. Di Renzo, F. Fajula, L. Mollo, B. Fubini and F. M. Ottaviani, *J. Colloid Interface Sci.*, 1998, **201**, 105.
- F. M. Ottaviani, A. Galarneau, D. Desplandier-Giscard, F. Di Renzo and F. Fajula, *Microporous Mesoporous Mater.*, 2001 **44–45**, 1.
- K. Edler, A. Goldar, A. V. Hughes, S. J. Roser and S. Mann, *Microporous Mesoporous Mater.*, 2001, **44–45**, 661.
- J. Patarin, B. Lebeau and R. Zana, *Curr. Opin. Colloid Interface Sci.*, 2002, **7**, 107.
- M. Tiemann, V. Goletto, R. Blum, F. Babonneau, H. Amenitsch and M. Lindén, *Langmuir*, 2002, **18**(26), 10053.
- K. Flodström, H. Wennerström and V. Alfredsson, *Langmuir*, 2004, **20**, 680–688.
- K. Flodström, C. V. Teixeira, H. Amenitsch, V. Alfredsson and M. Lindén, *Langmuir*, 2004, **20**, 10311–10316.
- (a) G. Friedel, *Colloid Chemistry*, The Chemical Catalog Co., New York, 1926, vol. 1, pp. 102–125; (b) F. B. Rosevear, *J. Am. Oil Chem. Soc.*, 1954, **31**, 628–639.
- (a) C. E. Fairhurst, S. Fuller, J. Gray, M. C. Holmes and G. J. T. Tiddy, *Handbook of Liquid Crystals*, 1980, **3**(7), 341; (b) S. Hassan, W. Rowe and G. J. T. Tiddy, in *Handbook of Applied Surface and Colloid Chemistry*, ed. K. Holmberg, John Wiley & Sons, New York, 2001, pp. 465–508.
- C. C. Egger, G. J. T. Tiddy, J. L. Casci and M. W. Anderson, in preparation.
- S. O'Brien, R. J. Francis, A. Fogg, D. O'Hare, N. Okazaki and K. Kuroda, *Chem. Mater.*, 1999, **11**, 1822.
- F. Babonneau, C. Toutou and S. Gaveriaux, *J. Sol-Gel Sci. Technol.*, 1997, **8**, 553.
- V. Gualandris, F. Babonneau, M. T. Janicke and B. Chmelka, *J. Sol-Gel Sci. Technol.*, 1998, **12**, 75.
- F. Babonneau and J. Maquet, *Polyhedron*, 2000, **19**, 315.
- B. Halle and H. Wennerström, *J. Chem. Phys.*, 1981, **75**(4), 1928.

- 26 A. Abragam, *Principles of nuclear magnetism*, Oxford Science Press, 1986, p. 239.
- 27 P.-O. Eriksson, G. Lindblom and G. Arvidson, *J. Phys. Chem.*, 1987, **91**(4), 846–853.
- 28 S. A. Buckingham, C. J. Garvey and G. G. Warr, *J. Phys. Chem.*, 1993, **97**, 10236–10244.
- 29 D. M. LeNeveu, R. P. Rand and V. A. Parsegian, *Nature*, 1976, **259**, 601–603.
- 30 L. J. Lis, W. T. Lis, V. A. Parsegian and R. P. Rand, *Biochemistry*, 1981, **20**, 1771–1777.
- 31 M. Carvell, D. G. Hall, I. G. Lyle and G. J. T. Tiddy, *Faraday Discuss., Chem. Soc.*, 1986, **81**, 223–237.
- 32 J. N. Israelachvili and H. Wennerström, *J. Phys. Chem.*, 1992, **96**, 520–532.
- 33 M. W. Anderson, C. C. Egger, G. J. T. Tiddy and J. L. Casci, *Studies in Surface Science and Catalysis*, 2002, **142**, 1149.